How will we move: Modeling Climate-driven Age-specific Displacement Migration

Mathew E. Hauer *
Department of Sociology, Florida State University
and
Sunshine Jacobs
Department of Sociology, Florida State University

July 1, 2021

Abstract

Global population projections show widespread ageing by century's end. The well-known relationship between age and migration propensity suggests more youthful populations are more likely to migrate than older populations. Yet relatively little research explores the important implication of ageing on human mobility in a changing climate, most likely driven by a paucity of migration data to comprehensively investigate the age structure of environmental migration. Here, we propose a displacement migration model to estimate age-specific migration probabilities. We combine a statistical outlier detection algorithm to first identify major environmental displacement events in US counties since 1980. Our findings suggests populations under age 60 are most likely to migrate after an environmental event, increasing with the size of displacement, validating many findings in the migration literature. We then build a flexible one-dimensional, age-specific displacement model based on these findings with estimation errors suggesting reasonable accuracy. Our proposed displacement model can be readily deployed to model prospective climate migration.

Keywords: Climate Change, Human Migration, Demography

*Thanks y'all!

1 Introduction

Environmental migration is an increasingly important concern in a warming world (Black et al. 2011, Findlay 2011, Boas et al. 2019). Some research suggests there could be as many as 140 million climate migrants by the middle of this century (Rigaud et al. 2018), suggesting environmental and climate migration will remain an important concern this century.

Although there is increasing interest in environmental migration, most migration research suffers from two key limitations. First, most studies on environmental migration use case study approaches employing either a single country or a single environmental event. Using case studies makes sense, especially with the ever lengthening list of major environmental events that can be coupled with good migration data. For instance, there are now a multitude of studies on Hurricane Katrina in New Orleans in 2005 (e.g., (Fussell et al. 2010, 2014, Thiede & Brown 2013, Groen & Polivka 2010)), a growing number of studies on Hurricane Maria in Puerto Rico in 2017 (Alexander et al. 2019, DeWaard et al. 2020, Acosta et al. 2020), and many studies on natural disasters (Kayastha & Yadava 1985, Loebach 2016, Paul 2005, Mallick & Vogt 2014). Few studies attempt more systematic analyses of environmental migration (see Obokata et al. (2014), Hunter et al. (2015), Hoffmann et al. (2020) for broader reviews of environmental). This has lead to a patchwork of our understanding of environmental migration, with environmental migration signals often showing conflicting findings (Hoffmann et al. 2020).

Second, most studies on environmental migration focus on population aggregates, examining total population changes (e.g. Lu et al. (2016), Hauer et al. (2020), Nawrotzki et al. (2013)). Yet migration propensity has a well-known age gradient where the most likely to migrate are young adults and the least likely are older adults. We know from some case studies that typical migration patterns manifest after an environmental event (Thiede & Brown 2013, Groen & Polivka 2010, Keenan & Hauer 2020), but these case studies involve some of the most destructive hurricanes in US history. The extent to which typical migration patterns manifest after smaller, less destructive events is presently unknown.

These two shortcomings related to isolated case studies and total population are important limitations on our ability to predict future environmental migration. The parallels between historic environmental migration and future climate migration form the backbone of most prospective analyses of climate migration (Rigaud et al. 2018, Hauer 2017, Chen & Mueller 2018, Xu et al. 2020). Yet many of these prospective analyses rely on individual case studies (Chen & Mueller 2018, Robinson et al. 2020), general migration theory (Hauer 2017, Bell et al. 2021), or heavy modeling of urban/rural populations (Rigaud et al. 2018, Gao & O'Neill 2020). Conspicuously missing from these models are attempts to capture the well-known relationship between migration propensity and age. Furthermore, while general migration theory and individual case studies are important and useful, the efficacy of using them for prospective analyses of climate migration is questionable.

In this article, we rectify these shortcomings of environmental migration studies. To overcome the limitation of case studies, we couple a statistical outlier (Chen & Liu 1993) technique with nearly 40 years of population data in approximately 3000 US counties (for approximately 120k county-years) to search for environmental events associated with large population declines. We then use the Spatial Hazard Events and Losses Database for the United States (SHELDUS)[1] to ensure the outliers we detect are associated with an environmental hazard rather than other factors, like a factory closing. This search provides a relatively large and varied historical pool of significant environmental hazards, overcoming the limitations of isolated case studies. From this pool of displacement events, we overcome the second limitation regarding a limitation to population aggregates by building a parsimonious, one-dimensional, age-specific displacement model. We link total population declines with changes in age-specific cohort change ratios to produce a predictive model of age-sex population changes in the face of an environmental hazard.

2 Environmental Migration

3 Methods

First, we describe the data sets we used. Second, the methodology for detecting statistical outliers in time series. Finally, we describe the creation of our flexible one-dimensional,

[1]available at `http://www.sheldus.org`

age-specific displacement model.

3.1 Data sets

We use two primary datasets: the National Vital Statistics System (NVSS) U.S. Census Populations with Bridged Race Categories data set[2] and the Spatial Hazard Events and Losses Database for the United States (SHELDUS).

The NVSS Bridged Race Categories data set harmonizes racial classifications across disparate time periods to allow population estimates to be sufficiently comparable across space and time. Importantly, all county boundaries are rectified to be geographically consistent across all time periods. We use the the 1969-2018 dataset which includes annual population estimates in five year age groups (0-4,..., 85+), two sex groups (male and female), and three race groups (White, Black, Other).

In our statistical outlier analysis (detailed below), we only consider counties created prior to 2000 and contained in the NVSS data. NVSS aggregated all counties in Hawaii to the state-level in the 1969-2018 NVSS bridged race data and we exclude them from our analysis. Several counties were created after 2000 (most notably is Broomfield County, Colorado). The 15 counties excluded from our analysis due to boundary changes or other reasons are Hoonah-Angoon Census Area AK 02105, Kusilvak Census Area AK 02158, Prince of Wales-Outer Ketchikan Census Area AK 02201, Skagway-Hoonah-Angoon Census Area AK 02232, Wrangell-Petersburg Census Area AK 02280, Adams County CO 08001, Boulder County CO 08013, Broomfield County CO 08014, Jefferson County CO 08059, Weld County CO 08123, Hawaii County HI 15001, Honolulu County HI 15003, Kalawao County HI 15005, Kauai County HI 15007, and Maui County HI 15009.

We use these data in two separate steps. In our statistical outlier analysis, we aggregate all county-level estimates into annual total population estimates for each county for the period 1969-2016. The historical population estimates prior to 1980 display unusual volatility, so we consider only the time periods 1980-2018. We use the NVSS population estimates disaggregated by age/sex to calculate cohort-change ratios, which we describe below.

[2]Data can be downloaded here: `https://seer.cancer.gov/popdata/download.html`

The second data source we use is SHELDUS. SHELDUS is a county-level hazard data set for the US which contains information about the direct losses (property and crop losses, injuries, and fatalities) caused by a hazard event (thuderstorms, hurricanes, floods, wildfires, tornados, flash floods, earthquakes, etc.) for the period 1960 to the present. We use this database to ensure the county time periods we identify as statistical outliers with population losses contain experienced an environmental hazard in that county-year. This is to ensure the outlier population losses that we detect are associated with a hazard rather than other forces, such as economic forces.

3.2 Statistical Outlier Detection

We use a statistical time series outlier detection algorithm (Chen & Liu 1993), implemented in the R programming language (R Core Team 2019) via the tsoutliers package (López-de-Lacalle 2019). This algorithm iteratively uses ARIMA models to 1) identify potential outliers and 2) refit the ARIMA with the outliers removed to produce a counter-factual time series. Here we briefly summarize and describe the method.

Often, the behavior of a time series can be described and summarized in ARIMA models. If a series of values, y_t^*, is subject to m interventions or outliers at time points $t_1, t_2, \ldots, t_m$ with weights ω then y_t^* can be defined as

$$y_t^* = \sum_{j=1}^{m} \omega_j L_j(B) I_t(t_j) + \frac{\theta(B)}{\phi(B)\alpha(B)} a_t \tag{1}$$

Where $I_t(t_j)$ is an indicator variable with a value of 1 at observation t_j and where the jth outlier arises,

$\phi(B)$ is an autoregressive polynomial with all roots outside the unit circle,

$\theta(B)$ is a moving average polynomial with all roots outside the unit circle,

and $\alpha(B)$ is an autoregressive polynomial with all roots on the unit circle.

We examine three types of outliers at time point t_m:

1. additive outliers (AO), defined as $L_j(B) = 1$;
2. level shift outliers (LS), defined as $L_j(B) = 1/(1 - B)$; and
3. temporary change outliers (TC), defined as $L_j(B) = 1/(1 - \delta B)$ where δ is equal to 0.7.

Colloquially, additive outliers arise when a single event causes the time series to unexpectedly increase/decrease for a single time period; level shift outliers arise when an event causes the time series to unexpectedly increase/decrease for multiple time periods; and temporary change outliers arise when an event causes the time series to unexpectedly increase/decrease with lingering effects that decay over multiple time periods.

An outlier is detected with the estimated residuals using a regression equation

$$\pi(B)y_t^* \equiv \hat{e} = \sum_{j=1}^{m} \omega_j \pi(B) L_j(B) I_t(t_j) + a_t \tag{2}$$

where $\pi(B) = \sum_{i=o}^{inf} \pi_i B^i$.

Equations 1 and 2 allow for an automatic detection of outliers iterated over a two-stage process.

In stage 1, outliers are located. First, an ARIMA model is fit to the time series using the `forecast` package in R (Hyndman et al. 2019, Hyndman & Khandakar 2008) where the best performing ARIMA model is selected based on the Bayesian information criterion (BIC). Next, the residuals from the forecast are checked for their significance using equation 2 where only outliers above a critical t-static are considered "true" outliers ($|\tau| \geq 4$; p-value < 0.000063). We chose this threshold to minimize the probability of committing a Type I error (or claiming an outlier is true when it is in fact not). Finally, two additional rules are implemented: If multiple outliers are detected at the same time point, only the most significant outlier is selected and if outliers of the same type at consecutive time periods are detected, only the outlier with highest t-statistic is selected.

In stage 2, outliers are removed from the time series and a new ARIMA model is chosen and fit. The selection of the initial ARIMA model could have been affected by the presence of the outliers, making some outliers spuriously identified. To correct for this, a new ARIMA model is fit accounting for additional regression effects in equation 1 from the list of candidate outliers identified in stage 1, effectively removing the outliers from the time series. Each outlier is then reassessed under the new model and those outliers that are no longer significant are removed.

These two stages are then iterated until no additional outliers are detected.

Figure 1 shows a toy example for outlier detection in a time series using the example of

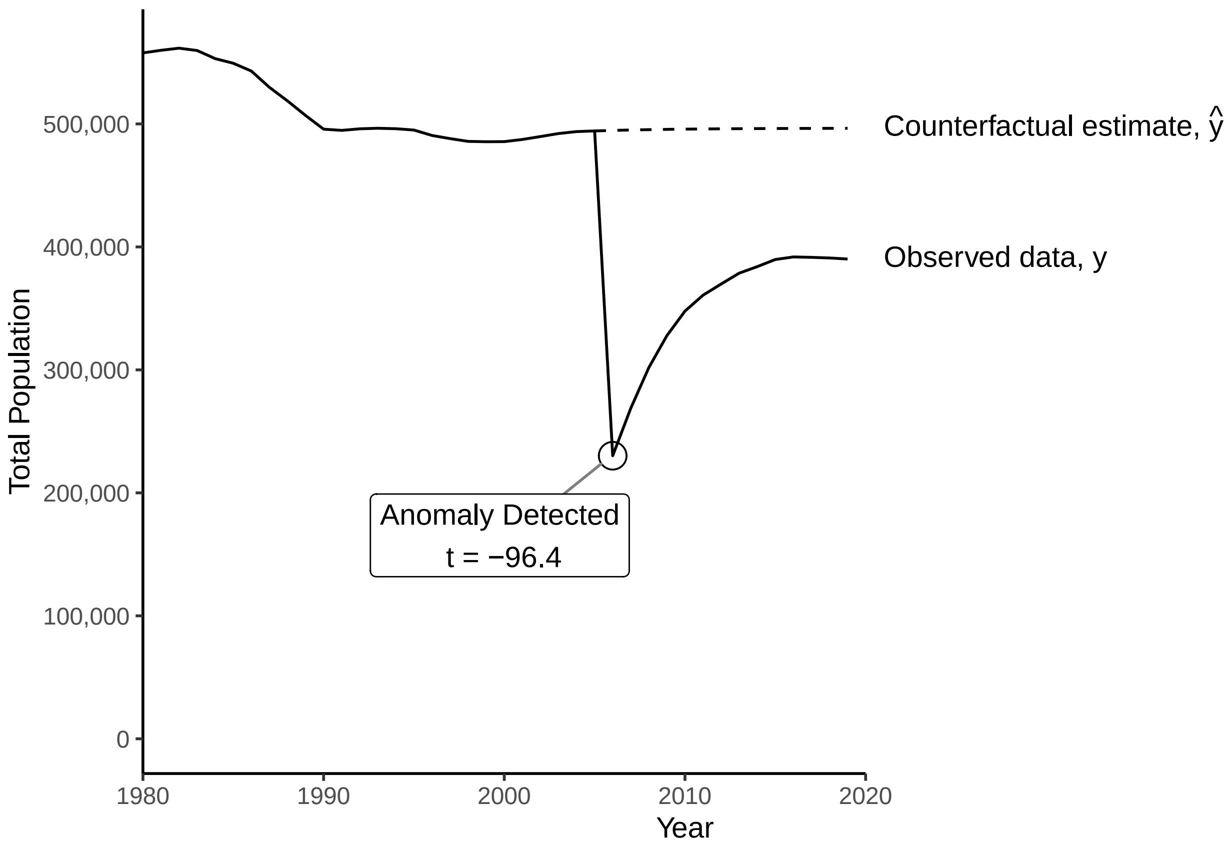

Figure 1: **An example of outlier detection using Hurricanes Katrina and Rita in Orleans Parish Louisiana in 2005.** Hurricane Katrina struck Louisiana in 2005 and we use it as a toy example to illustrate our approach. This figure shows the annual time series of total population in Orleans Parish between 1980 and 2019. Between 1990 and 2005, Orleans Parish total population changed from 495k to 494k, suggesting a possible 'plateau' in the population (illustrated with the dotted 'counterfactual'). Hurricane Katrina and the widespread population loss of more than 200k people represent a very strong outlier (t=-96.39).

Hurricane Katrina in Orleans Parish. On August 23 2005, Hurricane Katrina, a category 5 hurricane, struck southern Louisiana causing widespread damage and destruction in Orleans Parish in particular. The displacement from the Hurricane and the federal response were well documented (Hori et al. 2009, Fussell et al. 2014) and Census estimates suggest Orleans Parish lost more than 200,000 residents between 2005 and 2006. What would have been Orleans' population estimate had Hurricane Katrina *not* occurred? A simple counter-factual estimate might keep population size just under 500,000 people ($\hat{y}$).

In the Hurricane Katrina example, we have knowledge of the impact of Hurricane Katrina after the fact or ex-post-facto in order to create the counter-factual time series $\hat{y}$. But is this outlier detectable without knowledge of the Hurricane Katrina? In other words, can we detect the reduction of Orleans Parish's population between 2005 and 2006 using only the time series? Absolutely. The tsoutliers package identifies 2006 as an extremely strong level-shift outlier (t-stat = -96.39). The real world is hardly this simplified where a direct intervention is known, is large, and is testable. However, by using SHELDUS to verify environmental damages associated with large population declines, we can be confident the population shifts we detect are at least partially attributable to an environmental hazard.

3.3 Flexible one-dimensional, age-specific displacement model

We search all US counties for negative statistical outliers (indicating population losses) between 1980 and 2018. We detect population losses of magnitude 4σ or greater. We then searched the SHELDUS database to see if these county-years experienced per capita hazardous losses in excess of the 50th percentile. Four county-periods either were not in the SHELDUS database or experienced per capita hazard losses below the 50th percentile. Additionally, one county-period contained age-sex groups with 0 people, necessitating exclusion. These 48 environmental events include tornados, wind damage, winter weather, earthquakes, flooding, tropical cyclones, hail, and other environmental hazards.

With 48 county-periods exhibiting large population declines after verified hazard losses, across over nearly 40 years and across a wide variety of environmental hazards, we are able to overcome the first limitation of previous environmental migration modelling: that of isolated case studies of individual environmental events. With this large sample of environmental displacement, we next overcome the second limitation: that of only examining total population. To examine environmental migration across age, we build a flexible, one-dimensional, age-specific displacement model.

To link population displacement with age-specific population changes, we calculate cohort-change ratios in each county. Using the demographic accounting equation, the population at some time period t is equal to the $Pop_{t-1} + Births_{t-1} - Deaths_{t-1} + Migrants_{t-1,in} - Migrants_{t-1,out}$. For all age groups older than 0, $Births_{t-1}$ must be 0.

The calculation of a cohort-change ratio, as its name suggests, is relatively straightforward:

$$CCR_{x,t} = \frac{{}_nP_{x,t}}{{}_nP_{x-y,t-y}}$$

Where ${}_nP_{x,t}$ is the population aged x to $x+n$ in time t and ${}_nP_{x-y,t}$ is the population aged $x-y$ to $x+n-y$ in time t where y refers to the time difference between time periods. Since mortality must decrement a population, any CCR above 1.0 implies a net-migration rate in excess of the mortality rate, and a growing population.

We build the following model based on the relationship between the change in CCRs at age x, $\Delta CCR_x = CCR_{x,t}/CCR_{x,t-1}$, and the percentage decline in the total population compared to the counter-factual in the outlier detection method, $\Delta P_t = \hat{P}_t/P_t$:

$$log(\Delta CCR_x) = a_x + b_x h$$

Here, h is the $\log(\Delta P_t)$ and shows a linear relationship with the logarithm of the change in CCRs by age. x refers to five-year age groups: 0-4, 5-9,. . . , 85+. This is a similar model and approach to Wilmoth et al's (2012) flexible, one-dimensional mortality model based on the linearity between age-specific mortality rates and infant-mortality. **Table 1** depicts the correlation coefficients between $\log(\Delta CCR_x)$ and $\log(\Delta P_t)$. The age groups with the lowest correlation coefficients are young adult males aged 20-39 and those in the open-ended age interval (80+), suggesting these age/sex groups react to environmental signals the least predictably.

Figure 2 shows the relationship for selected age-groups between $\log(\Delta CCR_x)$ and

Table 1: **Correlation coefficients of changes in Cohort Change Ratios vs. Total Population Change (n=48).**

Age Group	Male	Female
0-4	0.931	0.944
5-9	0.954	0.934
10-14	0.963	0.965
15-19	0.806	0.930
20-24	0.650	0.919
25-29	0.710	0.934
30-34	0.752	0.959
35-39	0.874	0.975
40-44	0.936	0.964
45-49	0.971	0.963
50-54	0.969	0.977
55-59	0.965	0.958
60-64	0.896	0.888
65-69	0.809	0.912
70-74	0.937	0.826
75-79	0.839	0.795
80+	0.478	0.651

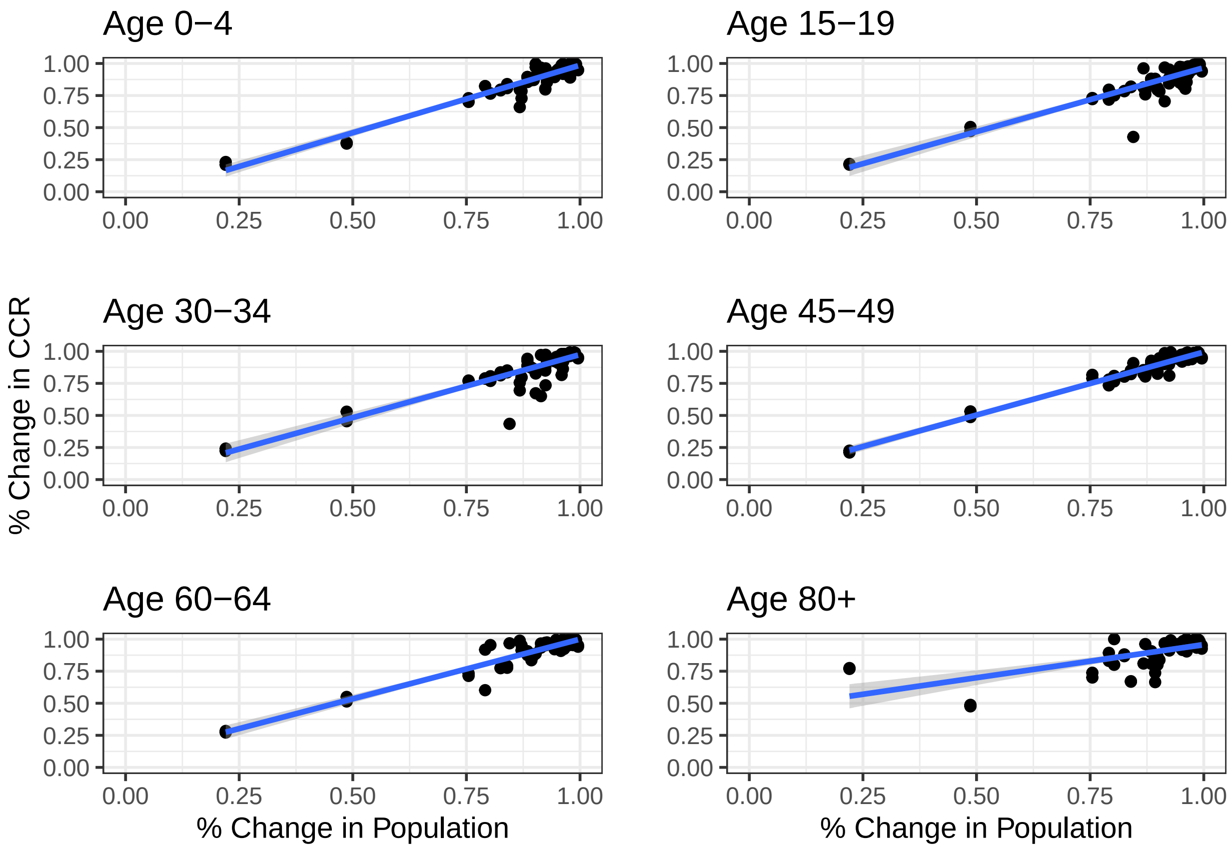

Figure 2: **Age-specific changes in cohort-change ratios (ΔCCR_x) vs. change in total population (ΔP_t).**

log(ΔP_t). Here we can see the near linear relationship between the percentage reduction in the population and the percentage reduction in CCR_x. Note the two county-years with the greatest reductions in total population refer to Louisiana counties most impacted by Hurricane Katrina.

3.4 Environmental Migration estimation using the fitted model

Using $h = log(\Delta P_t)$, we can estimate age-specific changes in CCRs after an environmental event by simply applying the following formula:

$$C\hat{C}R_{x,t} = CCR_{x,t-1} \cdot e^{\hat{\beta}_x h}$$

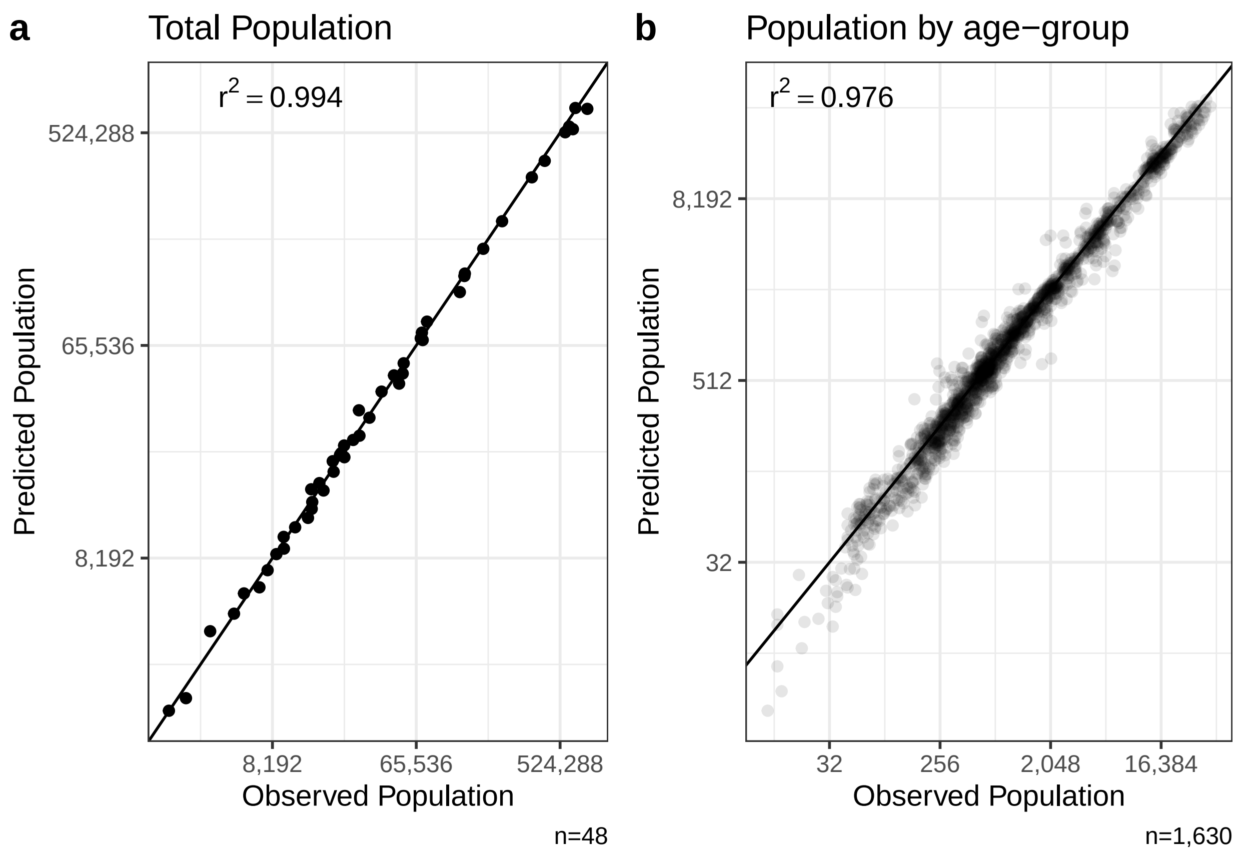

Figure 3: **Relationship between predicted populations using our model and observed populations in the 48 counties in our selection.** (a) shows the total population and (b) shows the populations for each age/sex group. The diagonal solid line is y=x. The model produces good fits for both the total population and by age/sex group.

Where $e^{\hat{\beta}_x h}$ provides the percentage change in CCR_x based on the $\log(\Delta P_t)$.In this case, we drop the intercept (a) from the estimation procedure to ensure a 0% decline in population yields a corresponding 0% change in the CCR. Simply multiplying the result from the model with the CCR in the year prior yields the anticipated change in the CCR. These changes in CCRs can then be applied to any time series of population values to generate an anticipated population.

Figure 3 shows the accuracy of the our fitted, one-dimensional model. We estimate the predicted population using the equation outlined above and then compare against the observed population. Regarding total population in our 48 counties, our model performs well with an r^2 value of 0.994 and performs well regardless of population size. Regarding each individual P_x group, our model performs slightly worse, but still performs quite well with an r^2 of 0.976. And just like with total population, the accuracy of our model does not depend on population size.

4 Conclusion

In this paper we introduced a flexible, one-dimensional age-specific migration model using a statistical outlier search algorithm. We searched over 3,000 US counties for significant population declines and then cross referenced our outliers with data from SHELDUS to eliminate spurious outliers. We then built and evaluated a predictive model of age-sex specific population change attributable to environmental events.

By using a more systematic analyses we are able to consider environmental migration clarifying the nature of environmental migration beyond individual case studies. Populations 60 and younger are more likely to migrate while those older than 60 could be demographically trapped.

We then built and evaluated a predictive model of age-sex specific population change attributable to environmental events allowing us to further analyze the possible displacement consequences of migration propensity and age. This displacement model predicts total population declines and the respective age/sex group changes.

The climate migration literature is replete with aggregate models of climate migration and displacement. However, our work underscores the importance of including basic demographic characteristics in prospective models of climate migration.

References

Acosta, R. J., Kishore, N., Irizarry, R. A. & Buckee, C. O. (2020), 'Quantifying the dynamics of migration after hurricane maria in puerto rico', *Proceedings of the National Academy of Sciences* **117**(51), 32772–32778.

Alexander, M., Polimis, K. & Zagheni, E. (2019), 'The impact of hurricane maria on out-migration from puerto rico: Evidence from facebook data', *Population and Development Review* **45**(3), 617–630.

Bell, A., Wrathall, D., Mueller, V., Chen, J., Oppenheimer, M., Hauer, M., Adams, H., Kulp, S., Clark, P., Fussell, E. et al. (2021), 'Migration towards bangladesh coastlines projected to increase with sea-level rise through 2100', *Environmental Research Letters* **16**(2), 024045.

Black, R., Bennett, S. R. G., Thomas, S. M. & Beddington, J. R. (2011), 'Climate change: Migration as adaptation', *Nature* **478**, 447–449.

Boas, I., Farbotko, C., Adams, H., Sterly, H., Bush, S., van der Geest, K., Wiegel, H., Ashraf, H., Baldwin, A., Bettini, G. et al. (2019), 'Climate migration myths', *Nature Climate Change* **9**(12), 901–903.

Chen, C. & Liu, L.-M. (1993), 'Joint estimation of model parameters and outlier effects in time series', *Journal of the American Statistical Association* **88**(421), 284–297.

Chen, J. & Mueller, V. (2018), 'Coastal climate change, soil salinity and human migration in bangladesh', *Nature Climate Change* **8**(11), 981–985.

DeWaard, J., Johnson, J. E. & Whitaker, S. D. (2020), 'Out-migration from and return migration to puerto rico after hurricane maria: evidence from the consumer credit panel', *Population and Environment* pp. 1–15.

Findlay, A. M. (2011), 'Migrant destinations in an era of environmental change', *Global Environmental Change* **21**, S50–S58.

Fussell, E., Curtis, K. J. & DeWaard, J. (2014), 'Recovery migration to the City of New Orleans after Hurricane Katrina: A migration systems approach', *Population and Environment* **35**(3), 305–322.

Fussell, E., Sastry, N. & VanLandingham, M. (2010), 'Race, socioeconomic status, and return migration to New Orleans after Hurricane Katrina', *Population and Environment* **31**(1), 20–42.

Gao, J. & O'Neill, B. C. (2020), 'Mapping global urban land for the 21st century with data-driven simulations and shared socioeconomic pathways', *Nature communications* **11**(1), 1–12.

Groen, J. A. & Polivka, A. E. (2010), 'Going home after hurricane katrina: Determinants of return migration and changes in affected areas', *Demography* **47**(4), 821–844.

Hauer, M. E. (2017), 'Migration induced by sea-level rise could reshape the US population landscape', *Nature Climate Change* **7**(5), 321–325.

Hauer, M. E., Holloway, S. R. & Oda, T. (2020), 'Evacuees and migrants exhibit different migration systems after the great east japan earthquake and tsunami', *Demography* **57**, 1437–1457.

Hoffmann, R., Dimitrova, A., Muttarak, R., Cuaresma, J. C. & Peisker, J. (2020), 'A meta-analysis of country-level studies on environmental change and migration', *Nature Climate Change* **10**(10), 904–912.

Hori, M., Schafer, M. J. & Bowman, D. J. (2009), 'Displacement Dynamics in Southern Louisiana After Hurricanes Katrina and Rita', *Population Research and Policy Review* **28**(1), 45–65.

Hunter, L. M., Luna, J. K. & Norton, R. M. (2015), 'Environmental dimensions of migration', *Annual Review of Sociology* **41**, 377–397.

Hyndman, R., Athanasopoulos, G., Bergmeir, C., Caceres, G., Chhay, L., O'Hara-Wild, M., Petropoulos, F., Razbash, S., Wang, E. & Yasmeen, F. (2019), *forecast: Forecasting*

functions for time series and linear models. R package version 8.10.
URL: *http://pkg.robjhyndman.com/forecast*

Hyndman, R. J. & Khandakar, Y. (2008), 'Automatic time series forecasting: the forecast package for R', *Journal of Statistical Software* **26**(3), 1–22.
URL: *http://www.jstatsoft.org/article/view/v027i03*

Kayastha, S. & Yadava, R. (1985), Flood induced population migration in india: a case study of ghaghara zone, *in* 'Population redistribution and development in south Asia', Springer, pp. 79–88.

Keenan, J. M. & Hauer, M. E. (2020), 'Resilience for whom? demographic change and the redevelopment of the built environment in puerto rico', *Environmental Research Letters* **15**(7), 074028.

Loebach, P. (2016), 'Household migration as a livelihood adaptation in response to a natural disaster: Nicaragua and hurricane mitch', *Population and Environment* **38**(2), 185–206.

López-de-Lacalle, J. (2019), *Tsoutliers: Detection of Outliers in Time Series*. R package version 0.6-8.

Lu, X., Wrathall, D. J., Sundsøy, P. R., Nadiruzzaman, M., Wetter, E., Iqbal, A., Qureshi, T., Tatem, A., Canright, G., Engø-Monsen, K. & Bengtsson, L. (2016), 'Unveiling hidden migration and mobility patterns in climate stressed regions: A longitudinal study of six million anonymous mobile phone users in Bangladesh', *Global Environmental Change* **38**, 1–7.

Mallick, B. & Vogt, J. (2014), 'Population displacement after cyclone and its consequences: Empirical evidence from coastal bangladesh', *Natural hazards* **73**(2), 191–212.

Nawrotzki, R. J., Riosmena, F. & Hunter, L. M. (2013), 'Do rainfall deficits predict us-bound migration from rural mexico? evidence from the mexican census', *Population research and policy review* **32**(1), 129–158.

Obokata, R., Veronis, L. & McLeman, R. (2014), 'Empirical research on international environmental migration: a systematic review', *Population and environment* **36**(1), 111–135.

Paul, B. K. (2005), 'Evidence against disaster-induced migration: the 2004 tornado in north-central bangladesh', *Disasters* **29**(4), 370–385.

R Core Team (2019), *R: A Language and Environment for Statistical Computing*, R Foundation for Statistical Computing, Vienna, Austria.
URL: *https://www.R-project.org/*

Rigaud, K. K., de Sherbinin, A., Jones, B., Bergmann, J., Clement, V., Ober, K., Schewe, J., Adamo, S., McCusker, B., Heuser, S. et al. (2018), 'Groundswell'.

Robinson, C., Dilkina, B. & Moreno-Cruz, J. (2020), 'Modeling migration patterns in the usa under sea level rise', *PloS one* **15**(1), e0227436.

Thiede, B. C. & Brown, D. L. (2013), 'Hurricane Katrina: Who Stayed and Why?', *Population Research and Policy Review* **32**(6), 803–824.

Wilmoth, J., Zureick, S., Canudas-Romo, V., Inoue, M. & Sawyer, C. (2012), 'A flexible two-dimensional mortality model for use in indirect estimation', *Population studies* **66**(1), 1–28.

Xu, C., Kohler, T. A., Lenton, T. M., Svenning, J.-C. & Scheffer, M. (2020), 'Future of the human climate niche', *Proceedings of the National Academy of Sciences* **117**(21), 11350–11355.